Dislocation depinning transition in a dispersion-strengthened steel

B. Bakó,[1,][*] D. Weygand,[2] M. Samaras,[1] W. Hoffelner,[1] and M. Zaiser[3]

[1]*Paul Scherrer Institute, 5232 Villigen PSI, Switzerland*

[2]*IZBS University of Karlsruhe, Kaiserstrasse 12, 76131 Karlsruhe, Germany*

[3]*Centre for Materials Science and Engineering, The University of Edinburgh, Edinburgh EH9 3JL, United Kingdom*

Discrete dislocation dynamics simulations are used to investigate the dynamics of a driven dislocation line interacting with randomly distributed, incoherent oxide dispersoids that act as pinning centers in a bcc ferritic alloy. The dislocation line undergoes a depinning transition where the order parameter is the mean dislocation line velocity v, which increases in the depinning region from zero as $v \sim (\tau - \tau_c)^\beta$ for external resolved shear stresses beyond a threshold value τ_c. The critical stress and critical exponents characterizing the depinning transition are determined numerically, and the observed dynamical behavior is compared with that of a depinning elastic string.

I. INTRODUCTION

The plastic deformation behavior of oxide dispersion strengthened steels is determined by interactions between lattice dislocations and dispersoids which lead to dislocation pinning and thus to an increased flow stress of the material. Particle strengthening by inclusion of precipitates, dispersoids, or both[1] is an extremely important mechanism used in technical alloys to improve their tensile and creep strengths.

Dispersoids strengthen the material by obstructing the motion of dislocations. However, due to the random arrangement and size distribution of the dispersoids it is not straightforward to predict the resulting flow stress increase. The general problem of the dynamics of dislocations interacting with randomly distributed obstacles has been studied as far back as the 1950s and 1960s (for a review of the early literature see Kocks *et al.*[2]). In recent years, discrete dislocation dynamics (DDD) simulations have become a powerful tool for studying microplasticity without requiring the simplifying assumptions inherent in earlier theoretical and simulation approaches. However, while DDD simulations can reliably predict the deformation behavior associated with specific configurations of obstacles, it is not *a priori* clear how to extrapolate the behavior of small simulated systems to that of the bulk material. Owing to the statistical nature of the obstacle distribution, flow stresses in small simulated systems may scatter and results of individual simulations may not be representative of bulk behavior. Moreover, it is not obvious whether the flow stress determined from a small simulation is likely to be too high (in a larger system, the dislocation might have more possibilities to circumvent or "unzip" strong obstacle configurations) or too low (a stronger configuration might be looming just behind the boundary of the simulation box). The naive answer to the problems of statistical scatter and finite-size effects is to make the simulation "big enough", but this raises the question on what big enough means. Within a one-off simulation, however large, there is no way to objectively assess and distinguish size-dependent and size-independent characteristics of the observed behavior.

It is therefore useful to look at the problem from a somewhat more theoretical point of view. Dislocations moving through random obstacle arrays are just one example of a more general problem: the driven motion of interfaces and elastic manifolds in random media. It is characteristic of these systems that an elastic manifold undergoes, upon an increase in the driving force, a depinning transition which separates a pinned "phase" where the manifold is asymptotically trapped in a metastable configuration and a moving phase where it asymptotically moves with nonzero velocity. This transition has been envisaged in analogy with standard critical phenomena,[3] with the driving force playing the role of a control parameter and the mean velocity of the manifold acting as the order parameter. At the critical value of the driving force, the velocity vanishes as $v \sim (\tau - \tau_c)^\beta$. Other examples of this kind of behavior include the electrical transport associated with charge-density waves,[4] driven flux motion in type-II superconductors,[5,6] domain walls in random-field Ising models,[7] and fluid invasion in porous media.[8]

II. MODEL

The theory of the depinning transition provides scaling relations that can be used to systematically extrapolate infinite system (bulk) behavior from finite simulations. In the present paper we use this idea to analyze the dynamics of an edge dislocation interacting with oxide dispersoids, which act as pinning centers in a bcc ferritic matrix, and to determine the corresponding increase in the critical resolved shear stress (CRSS) τ_c. We consider the overdamped dynamics of a single dislocation of average edge orientation, moving on its glide plane through a random obstacle field representing incoherent Y_2O_3 oxide dispersoids (ODS) with density and size distribution characteristic of PM2000, a commercial ferritic alloy of high deformation and creep resistance.[9]

The dislocation line is described by a set of nodes connected by straight segments. The evolution of nodal positions under the Peach-Koehler force is obtained by the simple Euler forward integration scheme.[10] The elastic anisotropy is neglected. The drag coefficient of the dislocation segments is assumed to depend on their orientation (characterized by the angle ψ between the Burgers vector and the segment direction vector) as

$$M(\psi) = M_s \cos^2 \psi + M_e \sin^2 \psi, \tag{1}$$

where M_s and M_e are the drag coefficients of pure screw and edge dislocation segments, respectively. The dislocation self-
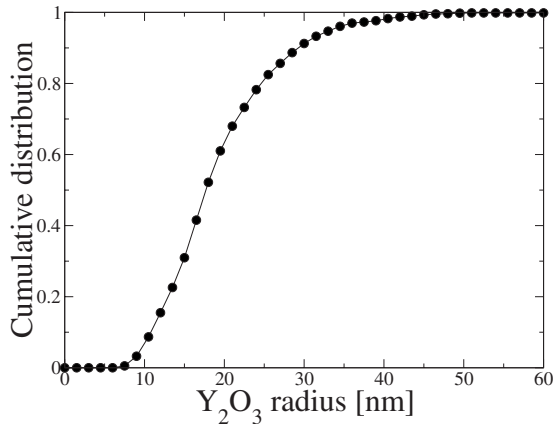
FIG. 1. Cumulative size distribution of Y_2O_3 particles determined from analysis of several TEM images.

interaction is described within the framework of linear elasticity in an infinite medium. The Y_2O_3 particles (with mean radius of 28 nm) are incoherent and impenetrable for the dislocations; therefore, they are modeled as hard-core spheres (i.e., the dislocation line cannot penetrate them). Their size distribution was determined experimentally by means of transmission electron microscopy (TEM) in conjunction with image processing techniques.[11,12] In the numerical model, particles with radii chosen randomly from the experimentally determined cumulative radius distribution function (Fig. 1) are placed randomly in three-dimensional (3D) space with uniform distribution and with the constraint that no particles overlap.[13]

III. RESULTS

To obtain the critical resolved shear stress τ_c, which is well defined only for systems of infinite size, many smaller systems with different realizations of the random dispersoid distribution are considered instead of studying a system as large as possible. The systems are of size $L \times L$ containing an initially straight edge dislocation line $x=0$ in the slip plane $z=0$, with the Burgers vector parallel to the x axis and line direction parallel to the y axis. Periodic boundary conditions are assumed in the y direction. Simulations for three different system sizes $L=2$, 3, and 4.5 μm were performed using the material parameters of the bcc Fe matrix: shear modulus μ =86 GPa, Poisson ratio of 0.291, and lattice constant of 0.287 nm. The drag coefficients the values of iron single crystal at room temperature measured by Urabe and Weertman:[14] 0.66 Pa s for screw and 0.345 Pa s for edge dislocation segments.

To determine the critical resolved shear stress τ_c of an infinite system, the size-dependent transition probability $P_L(\tau)$ is defined as the fraction of realizations where, for a given stress τ and in a system of size $L \times L$, the most advanced segment of the dislocation line initially placed at $x=0$ reaches the boundary of the simulation box at $x=L$. A scaling argument typical of the theory of critical phenomena is then used. For sufficiently large systems, the behavior of finite-size systems converges to that of an infinite system
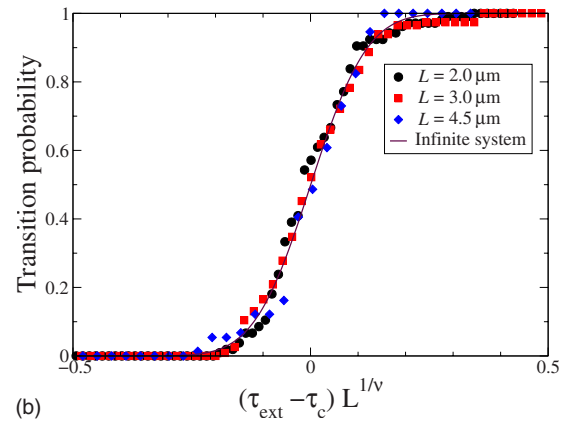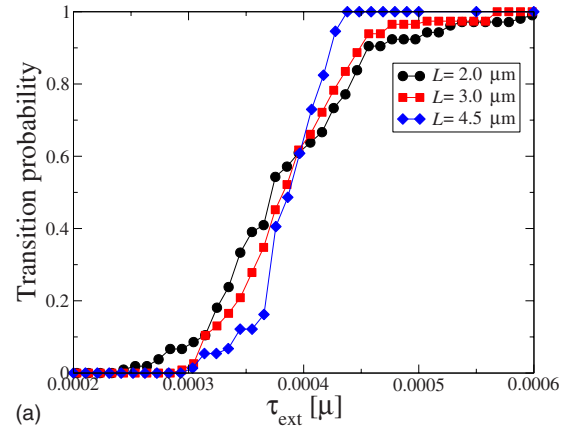

FIG. 2. (Color online) Transition probabilities $P_L(\tau)$ for different system sizes (top) and their finite-size-scaling collapse for $\tau_c = 385 \times 10^{-6} \mu$ and $\nu = 1.05$ (bottom); on the right, stresses are measured in units of μ and system sizes in units of nm.

according to specific scaling laws. Specifically, there exists an invariant distribution

$$P(\tilde{\tau}) = P_L[(\tau - \tau_c)L^{1/\nu}], \qquad (2)$$

which is asymptotically independent of L for $L \to \infty$. The exponent ν can be interpreted as a correlation length exponent. The existence of an invariant distribution provides us with a practical criterion to decide whether our system sizes are big enough. If parameters τ_c and ν are such that the distributions P_L obtained at several values of L collapse on top of each other, this indicates that the same parameters characterize the asymptotic behavior of the infinite system.

Transition probabilities $P_L(\tau)$ for different system sizes L are shown in Fig. 2 (left). The critical resolved shear stress τ_c and scaling exponent ν are obtained by simultaneously fitting the model function

$$P_L(\tau) = \frac{1}{2}\left[1 + \text{erf}\left(\frac{(\tau - \tau_c)L^{1/\nu}}{\sqrt{2}\sigma}\right)\right] \qquad (3)$$

to all $P_L(\tau)$ distributions determined from the different simulation series. This yields $\tau_c = (385.0 \pm 0.5) \times 10^{-6}\mu$ and $\nu = 1.05 \pm 0.05$. As can be seen from Fig. 2 (right), the corresponding invariant distribution gives a good representation of the finite-size distributions for all three investigated sys-
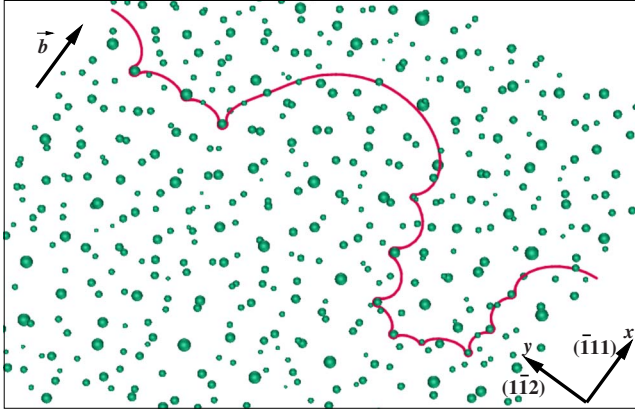
FIG. 3. (Color online) Typical pinned configuration close to the critical stress of an initially straight edge dislocation line (slip system $\frac{a}{2}(110)[\bar{1}11]$). Periodic boundary conditions in the $(1\bar{1}2)$ direction make the dislocation line infinitely long.

tem sizes. This indicates that the investigated system sizes, although limited, are indeed sufficiently large to capture the asymptotic approach toward the bulk behavior and that the numerical value of τ_c can be interpreted as the flow stress of the infinite system. Failure to obtain collapse would have been a definite signature of too small system size.

As the dislocation moves, its interaction with the pinning dispersoids leads to roughening. The dislocation line shape is characterized in terms of the displacement $h(y)$ measured from the initially straight line at time $t=0$. This may, however, not be a uniquely defined function as the dislocation may develop overhangs (see Fig. 3). In that case the displacement $h(y)$ is defined as the location of the most advanced segment for a given y. Then the line shape is statistically characterized in terms of the displacement-displacement correlation function

$$C(l,t) = \langle \overline{[h(y+l,t) - h(y,t)]^2} \rangle^{1/2}, \qquad (4)$$

where the overbar denotes the average over all y in a system of size L and the brackets denote an average over different
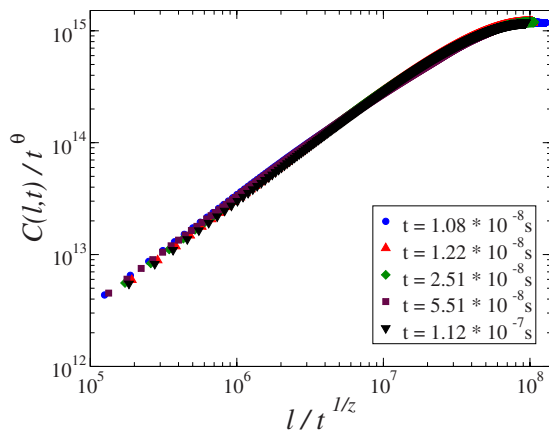

FIG. 4. (Color online) Data collapse of displacement-displacement correlation functions $C(l,t)$ obtained at $\tau \approx \tau_c$ for different times. Space is measured in units of lattice spacing and time in seconds. Data collapse is obtained for $z=1.32$ and $\theta=0.75$.
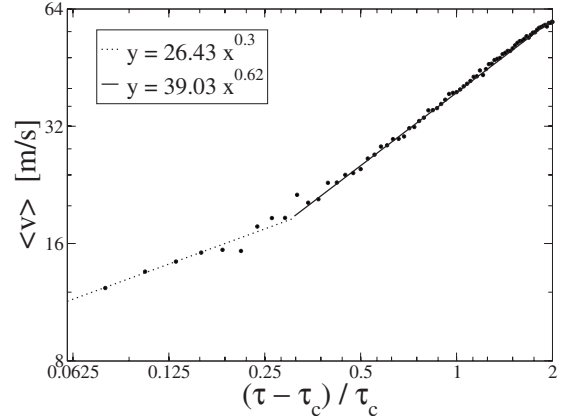

FIG. 5. Dislocation velocity v as a function of the excess driving stress beyond the threshold value τ_c.

realizations. At the critical stress τ_c, we expect the asymptotic shape of the depinning dislocation line to be characterized by self-affine roughness without any characteristic length: $C(l,\infty) \propto l^\zeta$ where ζ is the roughening exponent. The approach to this asymptotic shape is characterized by power-law behavior in both space and time, as expressed by the Family-Vicsek dynamic scaling ansatz[15]

$$C(l,t) \sim t^\theta f(l/t^{1/z}). \qquad (5)$$

Here, the function $f(u)$ increases as u^ζ for $u \ll 1$ and approaches a constant for $u \gg 1$. The exponent $\theta = \zeta/z$ is called the growth exponent.

The roughness and growth exponents can be determined by analyzing the evolution of the displacement-displacement correlation function at stresses close to the critical stress. Data collapse (Fig. 4) is obtained when $C(l,t)/t^\theta$ is plotted against $l/t^{1/z}$. The best fit is obtained for $\theta = 0.74 \pm 0.02$ and $z = 1.32 \pm 0.04$, resulting in a roughness exponent $\zeta \equiv z\theta = 0.98$. Direct determination of the roughness exponent from the slope of the displacement-displacement correlation function, averaged over 200 realizations of randomness, gives $\zeta = 0.96 \pm 0.02$. Successful scaling collapse requires that the local and global roughness exponents coincide.[16]

If depinning is envisaged as a critical phenomenon, the important quantity above the depinning threshold τ_c is the velocity exponent β which characterizes the increase in the dislocation velocity v with stress. The mean velocity of the dislocation line for constant driving stress can be obtained by tracking the position of the center of mass of the line, then performing a spatial average and an average over different obstacle configurations (Fig. 5). In the depinning region, v scales as $v \sim (\tau - \tau_c)^\beta$. For $L=2$ μm, the best fit close to the critical stress is obtained for $\beta = 0.30 \pm 0.05$, which then crosses over to an exponent of ≈ 0.6 for larger stresses.

IV. DISCUSSION

The critical exponents determined satisfy, within the statistical accuracy of the numerical values, the scaling relations

TABLE I. Summary of critical exponents. First- and second-order FRG results according to Le Doussal *et al.* (Ref. [19]) and simulation results for elastic line depinning according to Leschhorn *et al.* (Ref. [17]).

Exponent	FRG $O(\epsilon)$	FRG $O(\epsilon^2)$	Simulation (elastic line)	This work
ν	3/4	0.98	1.1 ± 0.1	1.05 ± 0.05
β	2/3	0.31	0.4 ± 0.05	0.03 ± 0.05
ζ	1	1.43	1.25 ± 0.05	0.96 ± 0.02
z	4/3	0.94	1.54 ± 0.05	1.32 ± 0.04

$$\frac{\beta}{z - \zeta} = \frac{1}{2 - \zeta} = \nu, \tag{6}$$

which are expected to hold for depinning manifolds.[17] It is therefore interesting to compare our exponent values with the results of simulations and functional renormalization-group (FRG) calculations for the depinning of a one-dimensional elastic manifold (an elastic string).[17–19] The comparison in Table I shows that our computer simulations yield critical exponents close to those for the depinning and viscous motion of an elastic string in a statistically isotropic, weakly disordered medium. At first glance this result seems to be unremarkable. After all, it is well known that self-interactions of a curved dislocation line can, with reasonable accuracy, be described in a line tension approximation, i.e., the dislocation behaves in this approximation like an elastic string. The long-range nature of the dislocation self-interaction leads only to logarithmic corrections to this picture. The line tension associated with a bulge in a straight dislocation line increases logarithmically with bulge radius.

However, there are a few notable differences between the situation considered in the present simulations and the bulk of theoretical and simulation work on elastic line depinning:

(i) All analytical and most of the simulation results have been obtained for the limit of weak pinning, where the collective action of many weak obstacles creates a Gaussian pinning "landscape." (In the context of dislocation pinning, this would correspond to the case of solution hardening.) In the present case, on the other hand, the dislocation is anchored at individual dispersoids which act as strong pinning points.

(ii) In published simulations of elastic line depinning, the individual segments are only allowed to move in the direction perpendicular to the average line direction. Hence, the possibilities of "sideways" motion and the formation of overhangs or loops are *a priori* excluded. This may not be a severe approximation for weak obstacle fields, but it is clearly impossible to apply a similar approximation to the present situation, where strongly pinned dislocations may develop significant overhangs as seen in Fig. 3.

(iii) Simulations of the depinning of elastic lines consistently yield "superrough" behavior with roughness exponents $\zeta > 1$.[17] Our simulations, on the other hand, suggest $\zeta \approx 1$ in line with the first-order FRG result shown in Table I. This finding is consistent with the result of a previous study of

dislocation depinning[20] which investigated a different obstacle field (a superposition of stress fields of threading dislocations leading to weak pinning), the description of the dislocation line (a screw-edge discretization), and the dynamics (a zero-temperature Monte Carlo simulation). The simulations have in common that long-range elastic self-interactions were considered and that lateral motion was allowed in both cases. Hence, the suppression of superrough behavior may be attributed to either of these factors.

In conclusion, the critical resolved shear stress τ_c and the critical exponents for the depinning of an edge dislocation in an alloy containing impenetrable obstacles have been calculated. The critical exponents determined indicate that the framework of depinning theory applies to this situation, even though corrections may be required to account for the influences of long-range self-interactions and the possibility of lateral dislocation motion in a strong pinning setting.

For simulation the obstacle distribution is taken to be characteristic of a PM2000 oxide dispersion strengthened ferritic alloy and the material parameters as characteristic for iron. For the investigated planar geometry in which only one dislocation is present, a depinning stress $\tau_c = 0.000385\mu \approx 34$ MPa is obtained. This value is significantly less than the recently measured critical resolved shear stress of 189 MPa for PM2000 single crystals deforming on $\{110\}\langle 111 \rangle$ slip systems.[21] To understand the discrepancy, it is important to note that real crystals contain a large number of dislocations of different slip systems. Such dislocation assemblies may form jammed configurations even in the absence of dispersoids. In addition, the PM2000 alloy contains high concentrations of randomly arranged aluminum (5.5 wt %) and chromium (19 wt %) atoms which provide additional contributions (solid solution strengthening) to the pinning landscape. Abundant propositions have been made in the metallurgical literature on how to add the pinning contributions of different types of obstacles and how to superimpose these on the self-jamming of mutually intersecting and interacting dislocation lines (for an overview, see, e.g., Kocks *et al.*[2]). However, these propositions remain essentially on the level of *ad hoc* rules without theoretical and often with scant experimental foundations. Even though some investigations have been devoted to the behavior of systems of straight dislocations,[22] a comprehensive theoretical and/or numerical investigation of the transition between stationary and moving phases in systems of mutually interacting dislocations is conspicuously lacking. This is true for the self-jamming of dislocations in the absence of other obstacles and even more so for the complex interactions between dislocation systems and random obstacle fields. Theoretical and experimental investigation of these problems therefore remains an exciting scientific task for future investigations.

*botond.bako@psi.ch

[1] A. S. Argon, *Physics of Strength and Plasticity* (MIT, Cambridge, MA, 1969).

[2] F. Kocks, A. S. Argon, and M. F. Ashby, Prog. Mater. Sci. **19**, 1 (1975).

[3] D. S. Fisher, Phys. Rev. B **31**, 1396 (1985).

[4] G. Grüner, Rev. Mod. Phys. **60**, 1129 (1988).

[5] A. I. Larkin and Yu. N. Ovchinikov, Sov. Phys. JETP **38**, 854 (1974).

[6] A. I. Larkin and Yu. N. Ovchinikov, J. Low Temp. Phys. **34**, 409 (1979).

[7] H. Ji and M. O. Robbins, Phys. Rev. B **46**, 14519 (1992).

[8] M. A. Rubio, C. A. Edwards, A. Dougherty, and J. P. Gollub, Phys. Rev. Lett. **63**, 1685 (1989).

[9] Dispersion-strengthened High-temperature Materials. Material Properties and Applications, Prospectus from Plansee, 706 DE.04.03(1000)RWF, 2003.

[10] D. Weygand, L. H. Friedman, E. Van der Giessen, and A. Needleman, Mater. Sci. Eng., A **309-310**, 420 (2001).

[11] B. Bakó, D. Weygand, M. Samaras, J.-C. Chen, M. Pouchon, P. Gumbsch, and W. Hoffelner, Philos. Mag. A **87**, 3645 (2007).

[12] B. Bakó, M. Samaras, D. Weygand, J. Chen, P. Gumbsch, and W. Hoffelner, J. Nucl. Mater. (to be published).

[13] A. Fuchs and D. Rönnpagel, Mater. Sci. Eng., A **164**, 340 (1993).

[14] N. Urabe and J. Weertman, Mater. Sci. Eng. **18**, 41 (1975).

[15] F. Family and T. Vicsek, J. Phys. A **18**, L75 (1985).

[16] J. M. López, M. A. Rodríguez, and R. Cuerno, Phys. Rev. E **56**, 3993 (1997).

[17] H. Leschhorn, T. Nattermann, S. Stepanow, and L.-H. Tang, Ann. Phys. (N.Y.) **6**, 1 (1997).

[18] P. Chauve, P. Le Doussal, and K. Wiese, Phys. Rev. Lett. **86**, 1785 (2001).

[19] P. Le Doussal, K. J. Wiese, and P. Chauve, Phys. Rev. B **66**, 174201 (2002).

[20] S. Zapperi and M. Zaiser, Mater. Sci. Eng., A **309/310**, 348 (2001).

[21] Jiachao Chen and W. Hoffelner, Paul Scherrer Institute, 5232 Villigen-PSI, Switzerland; (private communication).

[22] M. Zaiser, Adv. Phys. **55**, 185 (2006).